

Processing and Properties of PM 440C Stainless Steel

Prasan K. Samal, Joshua C. Valko, and Joseph D. Pannell
North American Hoganas, Hollsopple, PA 15935

ABSTRACT

Alloy 440C is a high carbon, hardenable, martensitic grade of stainless steel, which offers high wear resistance, combined with a moderate resistance to corrosion. A successful PM (powder metallurgy) version of the alloy should exhibit a high sintered density, at least greater than 7.60 g/cm^3 , i.e., above 98% of full theoretical density. Liquid phase sintering offers an attractive means of achieving this high density via single-press-single-sinter process. In addition, the sintered and heat treated material should have a predominantly martensitic matrix, with minimal amount of grain boundary carbides for achieving good impact strength.

The current paper covers the process parameters used, and the mechanical properties achieved, for a liquid phase sintered 440C alloy in both as-sintered and heat-treated conditions. The sintered density and hardness of this PM version of the alloy are comparable to those of the wrought and MIM (metal injection molding) processed 440C materials.

INTRODUCTION

Stainless steels are selected for a wide range of applications because of their superior resistance to corrosion and oxidation. For a vast majority of applications the strength requirements are rather moderate. Alloys from austenitic and ferritic families, with yield strengths ranging from 170 MPa to 310 MPa (25,000 to 45,000 psi), are therefore found to be satisfactory for a great many applications. For applications that require higher levels of strength and hardness, alloys from the martensitic family are frequently specified. These

alloys are heat treatable and, in comparison to the austenitic and ferritic grades, these can be processed to significantly higher hardness levels – with concomitant reduction in ductility. A large majority of martensitic stainless steels fall under two subgroups: low carbon, and high carbon martensitic stainless steels (two other subgroups, namely the low-carbon nickel bearing martensitic, and the medium-carbon martensitic, are less popular and are not well defined) [1]. The low carbon martensitics typically contain 0.10 to 0.20% carbon. In order to be heat treatable, the low carbon martensitic grades must be associated with lower chromium levels, generally ranging from 10.5 to 12.5%.

Low carbon martensitic stainless steels made via PM are typically used as bushings and wear plates. Single-press-single-sinter components of PM 410 and 420 typically exhibit sintered densities in the range of 6.5 to 6.8 g/cc [2]. These low sintered densities lead to lower wear resistance, hardness, and ductility, in comparison to their wrought counterparts. Thus, their use is significantly limited. Unlike the ferritic alloys, the martensitic stainless steels exist in the austenitic form at the sintering temperature. Since the atomic diffusion rates are slower in the austenitic matrix, in comparison to the ferritic matrix, a relatively small amount of shrinkage results during sintering. This makes it difficult to achieve sintered densities that are greater than 6.90 g/cm³ for most austenitic and martensitic stainless steels via solid state sintering.

The higher carbon containing alloys can remain heat treatable with the chromium content raised as high as 18.0%. Prominent among the high carbon martensitics is the alloy with the AISI designation 440. With a basic composition of 17% Cr, 1% Mo, and balance Fe, the alloy is divided into three sub-grades that differ in their carbon levels. Alloy 440A has a carbon content of 0.60 to 0.75%, the alloy 440B has a carbon content of 0.75 to 0.90%, and the alloy 440C has a carbon content of 0.95 to 1.20%. Alloys from both the high and the low carbon martensitic families are also available as free machining modifications.

Owing to a high hardness of HRC 56 to 60, the wrought and MIM versions of alloy 440C find use in applications that require good wear resistance, combined with a moderate corrosion resistance. Popular uses of the alloy include cutlery, food pressing/canning equipment, surgical and dental instruments, scissors, springs, valves, gears, shafts, propellers, cams, and ball bearings.

The annealed version of alloy 440C is not very popular since the hardness it offers is not unique and sensitization is unavoidable during the annealing process. Nevertheless, achievement of a relatively low annealed hardness (preferably to below HRC 20) is of significant importance when a wrought process is used. While the low formability of the alloy is seen as a major hurdle in the wrought processing of 440C components, it is of little concern in the case of MIM and PM processing because of their near-net shape capability. In order to capitalize on this advantage, the PM process must be capable of achieving full or near-full theoretical density in a cost effective manner. Once this obstacle is removed, PM based martensitic stainless steels can be cost effective in a variety of applications requiring high wear resistance.

It is therefore imperative that in order to make the PM route attractive for manufacture of high carbon grades of martensitic stainless steel achievement of full or near-full theoretical density is essential. Liquid phase sintering (transient) is well recognized as a convenient process route for achieving near-full theoretical sintered densities for many PM ferrous alloys. Achievement of near-full theoretical density can put PM 440C at par with the wrought and MIM processed versions of the alloy. The goal of this work was to demonstrate the feasibility achieving near-full density (>98% of theoretical full density) via liquid phase sintering and to determine its properties.

MATERIALS

The composition of 440C is similar to that of the alloy 434L, a popular ferritic grade of stainless steel with the exception that 440C has a much higher carbon content. This makes it convenient to produce the sintered version of 440C simply by adding graphite to a 434L powder. In this study, the powder mix comprised a standard, annealed grade of 434L powder, fine graphite, fine ferro-boron, and the lubricant lithium stearate, as shown in Table 1. Ferro-boron (18% boron) provided the boron necessary for promoting liquid phase sintering. The components were mixed in a Turbula blender for fifteen minutes. The 434L powder used was a commercially produced, water atomized powder. It was an annealed powder with a nominal particle size of minus 100 mesh (<149 μm). Table 2 lists the chemical composition and physical characteristics of the 434L powder used.

Table 1: 440C Powder mix (by weight %)

Annealed 434L powder – 97.90%
 Fine graphite powder – 1.35%
 Lithium stearate - 0.50%
 Ferro-boron powder - 0.25%

Table 2: Properties of 434L base powder used (weight %)

Alloy	Fe	Cr	Mo	Si	Mn	P	S	C	N	O	A D, g/cm ³	% <44 μm
434L	Bal	16.8	0.94	0.82	0.13	0.015	0.011	0.024	0.035	0.22	2.85	53

PROCESSING

In this study only two types of samples were used: Transverse Rupture Strength test (TRS) test bars and ‘dog bone’ tensile (flat bar) specimens, with dimensions as specified in MPIF Test Methods 41 and 10, respectively.

A compaction pressure of 758 MPa (55 TSI) was employed for production of both types of green specimens. This relatively high compaction pressure was selected with a view to minimize the shrinkage and distortion that typically occur during liquid phase sintering. The compacting properties of the 434L powder (base powder) and those of the 440C powder mix are shown in Table 3.

Table 3: Compacting properties of the powders

Powder	A. D. g/cm ³	Green density, g/cm ³	Green strength, MPa (PSI)	Carney flow rate, s/50 g
434L + 0.5% Li St	2.90	6.70	13.4 (1937)	6.8
440C Powder mix	2.60	6.55	16.7 (2426)	10.7

The green compacts were delubricated in a 100% hydrogen atmosphere, at a temperature of 538 °C (1000 °F) for 15 minutes. Sintering was carried out in a batch furnace under an atmosphere of 100% hydrogen. Three sintering runs were carried out. In the first sintering run, the sintering temperature was set at 1260 °C (2300 °F). Since this run did not produce the targeted sintered density, a second sintering run was carried out at a temperature of 1271 °C (2320 °F). The higher sintering temperature did yield the targeted sintered density of > 98% of theoretical full density (> 7.60 g/cm³). In the first and second sintering runs only TRS bars were processed. A third sintering run was carried out using the same sintering temperature as the second one, where both the ‘dog bone’ tensile specimens and the TRS bars were sintered. The heat up rate, soak times, hold times, and the cooling rates were kept the same in each of the three sintering runs. The average cooling rate from the sintering temperature to 538 °C (1000 °F) was 0.70 °C/sec. (1.26 °F/sec.).

A number of samples were tested in the as-sintered condition for sintered density, hardness, yield strength, U.T.S., and elongation. Sintered samples were analyzed for carbon, oxygen, and nitrogen contents.

A number of sintered samples were heat treated for maximizing hardness. Heat treatment was carried out at Blue Water Thermal Services, South Bend, IA. The samples were soaked at 1052 °C (1925 °F) in vacuum for 20 minutes, followed by air quenching. Immediately following air quenching the samples were given a sub-zero cooling (less than -75 °C, -103 °F) to convert any remaining retained austenite to martensite. A set of ‘dog bone’ tensile specimens were given a tempering treatment at 163 °C (325 °F) for 30 minutes. All hardness and tensile testing was carried out at Chicago Spectro Services Laboratory, Inc., Chicago, IL. Metallographic evaluation was made on the as-sintered and the heat treated samples.

RESULTS AND DISCUSSION

Table 4 shows the sintered properties of samples produced in each of the three sintering runs. The sintered densities of the samples produced in the first sintering run were lower than the minimum target of density of 7.60 g/cm³. Except for hardness determination, no further testing was carried out on these samples. The sintered densities of the samples processed in the second and third sintering runs did meet the desired value, and hence, these samples were utilized for further evaluation.

The typical carbon content of the sintered and heat treated samples was 1.04%. The typical oxygen content of the sintered and the heat treated samples was 730 ppm. The typical nitrogen content of the sintered and the heat treated samples was 25 ppm. The linear shrinkages of samples from the second and third sintering runs ranged from 5.0 to 5.5%.

Table 4: Sintered properties

Sintering run no	Sintering temperature, °C (°F)	Sintered density, g/cm ³ (% of theoretical density)	As-sintered hardness, HRC
1	1260 (2300)	7.35 to 7.55 (94.8 to 97.4)	20 - 23
2	1271 (2320)	7.67 to 7.72 (99.0 to 99.6)	39 - 42
3	1271 (2320)	7.65 to 7.72 (98.7 to 99.6)	39 - 41

The sintered densities of the 1271 °C (2320 °F) sintered samples ranged from 98.7 to 99.6% of theoretical full density. The hardness of the as-sintered samples (HRC 39 to 42) are higher than those of the fully annealed wrought 440C material (HRC 20 to 30). This is most likely the result of the relatively fast cooling rate used in these sintering runs, leading to some martensite formation. The cooling rate used for annealing wrought 440C is typically 0.007 °C/sec (0.013 °F/sec), which is one hundred times slower than the cooling rate employed here [3].

Table 5 compares the mechanical properties PM 440C with those of wrought and MIM versions of the alloy. The hardness of the heat treated and tempered PM 440C is very close to those of the wrought heat treated and tempered 440C (HRC 56 to 59 vs. HRC 57 to 60). The as-quenched PM 440C also has a very similar hardness. The as-sintered hardness of PM 440C (HRC 39 to 42) is unique, being significantly higher than that of solid state sintered PM 420 (HRC 20 to 30) [2].

The PM 440C exhibits higher U.T.S. and yields strength than the MIM 440C. The sintered density of the MIM material quoted here is lower than that of the PM 440C. The U. T. S. and the yield strength of the as-sintered PM 440C samples fall in between those of the annealed and the fully heat treated wrought 440C. The ductility of the as-sintered PM material is lower than that of the wrought-tempered 440C. Upon heat treatment the U.T.S. and yield strength of PM 440C fall in the lower end of the range of properties of the wrought heat treated 440C. The ductility of PM 440C is markedly improved by the heat treatment.

Table 5: Mechanical properties comparison

Material	Metallurgical condition	Sintered density, g/cm ³	Hardness HRC	U T S, MPa (KSI)	Yield strength, MPa (KSI)	Elong, %
440C - This study	As-sintered	7.70	39 - 42	738 (107)	730 (106)	1.0
440C – This study	Heat treated -As Quenched	7.70	56 - 58	N A	N A	NA
440C – This study	Heat treated & Tempered	7.70	56 - 59	752 (109)	710 (102)	2.8
Wrought 440C [1,4]	Heat treated & Tempered	7.75	57 - 60	896 - 1930 (130 - 280)	620 - 1860 (90 - 270)	1.0 - 2.0
MIM 440C [5]	Heat treated & Tempered	7.50	43	620 (90)	410 (59.5)	2.0

The results of the mechanical testing could have been affected by the small amount of distortion that the 'dog bone' specimens underwent during sintering, as well as by the surface roughness of the sintered specimens. This may partly account for the lower U.T.S. and yield strength of the PM 440C material in comparison to its wrought counterpart. A more reliable method of determining the mechanical properties would be to use machined and ground tensile test specimens with a smooth surface finish.

Microstructure

Figures 1 and 2 show the microstructure of the as-sintered PM 440C material having a sintered density of 7.70 g/cm^3 . The amount and the size of the residual porosity are small. This etched (Glyceresia) sample shows small carbide precipitates in a predominantly martensitic matrix. The carbide precipitates that are present within the grains are primary carbides, and are most likely of the M_{23}C_6 type. The carbides found along the grain boundaries (which incidentally are fewer) are secondary carbides of the type M_7C_3 that most likely formed during cooling. The volume fraction of the secondary carbides is much smaller when compared to the volume fraction of the primary carbides. No eutectic lamellar precipitates are noted at the grain boundaries (including pore-grain boundary triple points). This is because of the relatively small amount of boron (400 ppm, approx.) used in this study. Typically, in the liquid phase sintering of Cr containing alloys a high boron content leads to the formation of Cr-rich eutectic precipitates in the grain boundaries, and these can contribute to their brittleness [6]

Figure 3 shows the microstructure of the heat treated (as-quenched) material. In comparison to the microstructure of the as-sintered material, its matrix consists of a much coarser martensite.

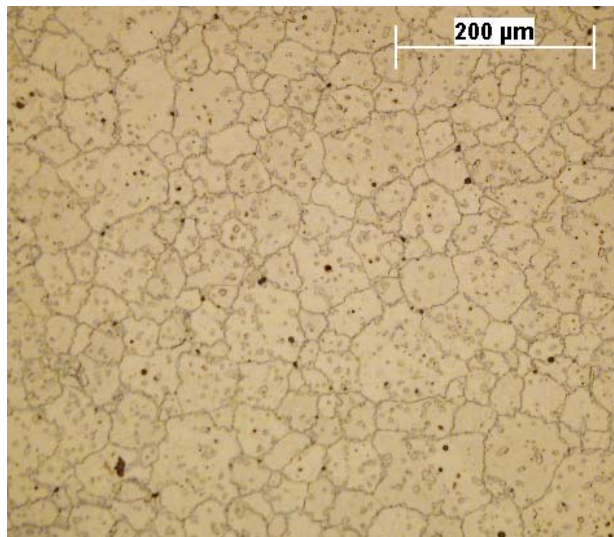


Figure 1: Microstructure of as-sintered PM 440C at a low magnification showing the presence of carbides in a matrix of fine martensite. Glyceresia etch.

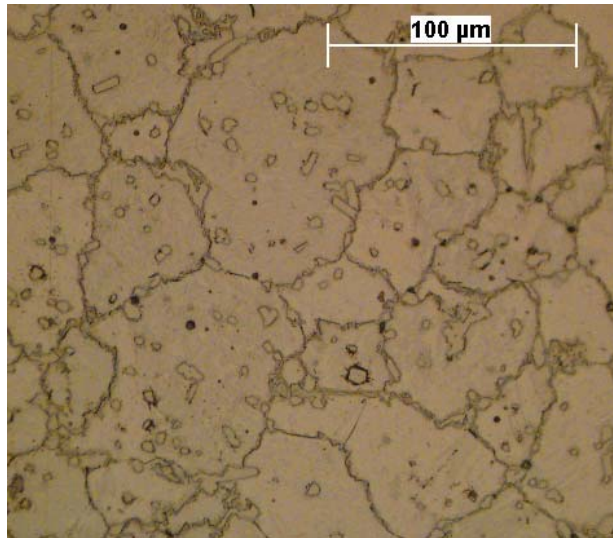


Figure 2: Microstructure of as-sintered PM 440C at a higher magnification. Glyceregia etch.

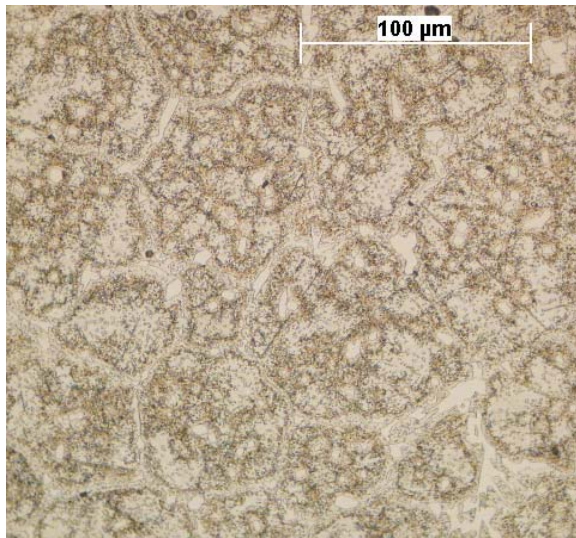


Figure 3: Microstructure of heat treated (as-quenched) PM 440C, showing carbide precipitates in a coarse martensitic matrix. Glyceregia etch.

The selection of the initial sintering temperature (1260 °C, 2300 °F) in this study was based upon data published by earlier researchers on liquid phase sintering of stainless steels.

While published literature on liquid phase sintering of the austenitic alloy 316L is numerous, only a limited amount of information is found in the literature on liquid phase sintering of ferritic and martensitic grades of stainless steels. In the authors' experience attempts to liquid phase sinter Mo-free ferritic alloys such as 410L and 409L have been problematic, yielding erratic results.

Toennes et al. were successful in liquid phase sintering a low chromium martensitic stainless steel by boron addition. The alloy was AISI grade 422, and it had a composition of 12.1% Cr, 0.98% Mo, 0.31% V, 0.23% C, 0.70% Ni, and 0.27% Si [7]. They determined that a minimum boron content of 200 ppm was essential for effective liquid phase sintering. The sintered density achieved was 7.70 g/cm^3 , and the sintering temperature was $1350 \text{ }^\circ\text{C}$.

Work by Sarasola et al. shows that Mo plays a critical role in the liquid phase sintering of boron doped ferrous alloys. By water quenching Fe-B and Fe-Mo-B samples from selected sintering temperatures and then by carefully examining their microstructures, they concluded that in the presence of Mo (0.5 to 1.5 wt. %), Mo containing borides of the type $(\text{Fe, Mo})_2\text{B}$ form in the alloy matrix at temperatures much lower than the " $\text{Fe}_2\text{B} + \text{Fe} \rightarrow \text{L}$ " eutectic ($1175 \text{ }^\circ\text{C}$, $2147 \text{ }^\circ\text{F}$), beginning at $1000 \text{ }^\circ\text{C}$ ($1832 \text{ }^\circ\text{F}$). These precipitates first form on the prior particle boundaries, and subsequently in the pores and grain boundaries. Not only the temperature for liquid phase formation is raised, but also when the eutectic liquid from the reaction " $(\text{Fe, Mo})_2\text{B} + \text{Fe} \rightarrow \text{L}$ " does form a significantly enhanced wetting of the solid phase occurs. Kirkendal pores formed due to the earlier diffusion of Mo and B become closed at the higher sintering temperature. This phenomenon may explain the relative ease with which near-full theoretical density was achieved in the current study.

Since the formation of the Mo rich borides occurs by solid state diffusion at a relatively low temperature, it is very likely that the heating rate leading up to the sintering temperature, as well as any inter-mediate hold temperatures and time, would significantly influence the outcome of the process. A more rapid heating rate or a shorter intermediate temperature hold period would very likely inhibit the formation of Mo containing borides, thus promoting Cr_2B formation. Liquid phase generation by the eutectic reaction of Cr_2B would occur at a lower temperature, which may be inadequate from the pore closure point of view. In addition, wetting of the solid phase by the Mo-free liquid would be less effective.

Liquid phase sintering is associated with large amounts of shrinkage, and some amount of distortion is inevitable due to non-uniform dimensional change. In the current study, a small degree of 'picture framing' was observed. With this type of distortion, the edges of the sample have a slightly greater thickness compared to the body. This phenomenon has been reported by earlier researchers in the liquid phase sintering of 316L [9.10]. Figure 4 compares the appearance of liquid phase sintered samples of this study with those of a reference sample (solid state sintering). In the current study, the edges of the as-sintered TRS bars were thicker than the body by 0.15 mm, (0.006 in.; or 2.5 % thicker). Despite the difficulty of controlling dimensional tolerances, the economics of this near-net shape process offers an attractive alternative to the wrought and MIM processing methods.



Figure 4: Images of 440C TRS bars (right four) showing the amount of distortion that occurred during liquid phase sintering. TRS bars (two) on the left side were produced from a stainless steel powder by conventional solid state sintering.

CONCLUSIONS

1. Liquid phase sintering of boron doped 440C powder mix is capable of producing near-full theoretical sintered densities (>99%).
2. The as-sintered PM 440C has a hardness in the range of HRC 39 to 42, and upon heat treatment its hardness increases to HRC 56 to 59, which is comparable to that of wrought heat treated 440C.
3. The sintering parameters, including the heat up rate, intermediate hold temperature, sintering temperature, sintering time, and the cool down rate must be carefully controlled in order to achieve the targeted sintered density and hardness.

REFERENCES

1. R. A. Lula, *Stainless Steel*, American Society for Metals, Metals Park, OH, 1986, pp 37 - 39.
2. M. Svilar and H. D. Ambs, PM Martensitic Stainless Steels: Processing and Properties. *Advances in Powder Metallurgy*, ed. E. Andreotti, P. McGeehan Vol 2, MPIF, Princeton, NJ, pp 259 - 272.
3. R. Kern, "Annealing 440C Stainless to Below HRC 30", *Heat Treating*, August 1992, Materials Park, pp 116.
4. J. R. Davis (Ed.), ASM Specialty Handbook *Stainless Steel*, ASM International 1994, pp 7 - 10.

5. R. M. German and A. Bose, *Injection Molding of Metals and Ceramics*, MPIF, Princeton, NJ, 1997, pp 10-294.
6. L. R. Jensen, "Liquid Phase Sintered Stainless Steel Based PM Metal Matrix Composites with CrB", *Proceedings of PM World Congress*, June 6-9, 1994, Paris, EPMA, vol. II, pp 1541 -1544.
7. C. Toennes, P. Ernst, G. Meyer, and R. M. German, " Full Density Sintering by Boron Addition in a Martensitic Stainless Steel", *Advances in Powder Metallurgy and Particulate Materials*, ed. J. M. Capus and R. M. German, 1992, vol 3 (Sintering) MPIF, Princeton, NJ, pp 371- 381.
8. M. Sarasola, T. Gomez-Acebo, and F. Castro, "Liquid Generation During Sintering of Fe-3.5% Mo Powder Compacts with elemental Boron Addition", *Acta Materialia*, 52 (2004), ELSEVIER, pp 4615 – 4622.
9. Molinari, J. Kazior, F. Marchetti, R. Canteri, I. Cristofolini, and A. Tiziani, " Sintering Mechanisms of Boron Alloyed AISI 316L Stainless Steel", *Powder Metallurgy*, vol 37 (No 2) 1994, pp 115 -122.
10. P. K. Samal and J. B. Terrell, „Effects of Boron Addition on the Corrosion Resistance of PM 316L Stainless Steel, *P/M Science and Technology Briefs*, vol. 3 (No 3) 2001, MPIF, Princeton, NJ, pp 18 - 24.